The Binary System Isotactic Polypropylene/ Bis(3,4-dimethylbenzylidene)sorbitol: Phase Behavior, Nucleation, and Optical Properties

Magnus Kristiansen, Michael Werner, Theo Tervoort, and Paul Smith*

Department of Materials, Eidgenössische Technische Hochschule (ETH) Zürich, CH-8092 Zürich, Switzerland

Markus Blomenhofer and Hans-Werner Schmidt

Macromolecular Chemistry I, and Bayreuther Institut für Makromolekülforschung (BIMF), Universität Bayreuth, D-95440 Bayreuth, Germany

Received February 28, 2003; Revised Manuscript Received April 28, 2003

ABSTRACT: The phase behavior of the binary system consisting of the commercial nucleating and clarifying agent 1,3:2,4-bis(3,4-dimethyldibenzylidene)sorbitol (DMDBS, Millad 3988) and isotactic polypropylene (*i*-PP) was investigated over the entire concentration range by means of differential scanning calorimetry (DSC), rheology, and optical microscopy. Experimental phase diagrams were constructed from data obtained in melting and crystallization studies, and a simple binary monotectic is advanced. Distinct regimes in the phase diagram, which apparently dictate nucleation and clarification of *i*-PP by DMDBS, are discussed. A maximum increase in the crystallization temperature of *i*-PP due to the nucleating action of DMDBS was observed in compositions containing between 0.2 and 1 wt % of the latter. Liquid−liquid phase separation was observed at elevated temperatures for *i*-PP/DMDBS mixtures comprising more than 2 wt % of DMDBS. A study of the optical properties of the *i*-PP/DMDBS system revealed that values for haze and clarity of injection-molded plaques progressively decreased and increased, respectively, in the concentration range between 0.2 and 1 wt % DMDBS in *i*-PP; at DMDBS concentrations exceeding 1 wt % the presence of the additive had an adverse effect on the optical properties of *i*-PP. Finally, a surprisingly strong influence of cooling kinetics on the phase behavior and, consequently, on the optical properties of the *i*-PP/DMDBS system was detected, which is of obvious relevance for industrial applications.

1. Introduction

Sorbitol derivatives such as 1,3:2,4-dibenzylidenesorbitol (DBS, Millad 3905, Milliken Chemical and Irgaclear D, Ciba Speciality Chemicals), 1,3:2,4-bis(*p*-methylbenzylidene)sorbitol (MDBS, Millad 3940, Milliken Chemical and Irgaclear DM, Ciba Speciality Chemicals), 1,3:2,4-bis(*p*-ethylbenzylidene)sorbitol (EDBS, NC-4, Mitsui Chemical), and bis(3,4-dimethylbenzylidene)-sorbitol (DMDBS, Millad 3988, Milliken Chemical) belong to a group of remarkably efficient nucleating agents for (the α-crystal form of) isotactic polypropylene (*i*-PP),[1] and addition of only small amounts (∼0.2 wt %) of certain of these compounds may also dramatically enhance the clarity and reduce haze of the solid polymer (hence the often-used denotation "clarifiers").[2,3] In contrast to most classical nucleating agents discussed in the literature (cf. ref 4), sorbitol derivatives are designed to dissolve in the molten polymer during processing to facilitate and enhance their dispersion. Upon cooling, the sorbitol compounds are reported to crystallize into nanofibrillar structures, yielding a 3-dimensional network in the polymer melt[3] as evidenced by an initial increase in viscosity prior to the solidification of the polymer itself.[5,6] In this context, the term "physical gelation of the polymer melt" has been used (cf. ref 2). The above sorbitol derivatives have been shown to be able to gel also various other polymer melts such as poly(dimethylsiloxane),[7] poly(propylene oxide),[8] poly-(propylene glycol),[9,10] polystyrene, and polycarbonate[11] as well as a variety of small molecular organic liquids[12−14] and liquid crystal mixtures[15] at truly remarkable low concentrations (typically below 0.5 wt %).

The nucleating ability of the above sorbitol derivatives has received and continues to attract considerable interest (e.g., refs 16−20), and a number of possible mechanisms have been proposed. For instance, it has been suggested that the efficient nucleation of *i*-PP by these compounds is promoted by the diameter of the crystallized additive fibrils (∼10 nm), matching the lamellar thickness of the polymer crystals[3] and by their extremely large surface resulting from the very fine size of the solid nucleating agent. In addition, certain epitaxial relationships between the sorbitol compounds and *i*-PP have been invoked (for instance refs 21 and 22).

Remarkably, the pronounced *clarifying* effect that particular sorbitol derivatives impart when dispersed in *i*-PP has received relatively little attention. Equally surprising, the phase behavior of these sorbitol derivatives and *i*-PP has been investigated primarily in the low additive concentration range (i.e., <1 wt %). Of course, the latter clearly is of most commercial relevance since (ideally) very small amounts of nucleating and clarifying agents are used, among other things, to avoid possible deteriation of mechanical properties of the polymer. However, examination of only this part of the phase diagram may not provide sufficient information to deduce the underlying principles leading to the dramatic optical effects that the minor amounts of these clarifying agents may cause, which could permit devel-

10.1021/ma030146t CCC: $25.00
Published on Web 06/13/2003

opment of guidelines for the design of other effective species. Hence, in this paper we present a detailed study of the phase behavior of the system *i*-PP/DMDBS over the entire concentration range and discuss its relevance to the observed clarifying phenomenon.

2. Experimental Section

Materials. The *i*-PP grade used was Montell FLF20 (M_n = 5.45 × 10^4 g/mol, M_w = 3.77 × 10^5 g/ mol), which contained the antioxidant Irganox 1010. (Hence, strictly speaking, the present *i*-PP/DMDBS system is a pseudobinary.) Prior to use, the polymer pellets were pulverized in a freezer mill (Retsch ZM100, Schieritz & Hauenstein AG, Switzerland). The nucleating agent bis(3,4-dimethylbenzylidene)sorbitol (DMDBS, Millad 3988, Milliken Chemical, Belgium) was used as received.

Sample Preparation. Various dry-blended mixtures of *i*-PP and DMDBS with DMDBS contents ranging from 0.1 to 20 wt % were compounded in a laboratory, corotating mini-twin-screw extruder (Technical University Eindhoven, The Netherlands) at 230 °C under a nitrogen blanket for 15 min, after which the mixtures were discharged. Samples for rheological analysis were prepared by conventional melt-compression molding at 240 °C of the above mixtures, yielding sheets of 1 mm thickness (molding time 10 min). Films for optical microscopy studies were prepared by compression-molding a granule of mixed material between two glass slides at 240 °C and subsequent quenching. Samples of higher concentrations of DMDBS (>40 wt %) were prepared by compression-molding powdered mixtures between two glass slides and heating at 240 °C for 10 min. It should be noted that concentrations hereafter reported refer to the respective initial weight fraction of the additive in the sample. Deviations from these initial concentrations may have developed during processing due to degradation or sublimation of some DMDBS, which would somewhat affect the accuracy of the temperature/composition diagrams, especially in the low additive concentration regime.

Injection Molding. Samples for optical characterization were prepared by melting previously compounded mixtures for 5 min at 260 °C and subsequent injection molding using a microinjector (DACA Instruments, Goleta, CA), yielding plaques of 1.1 mm thickness and 25 mm diameter.

Optical Properties. The standard (industrial) optical characteristics haze and clarity were measured for the above injection-molded disks with a "Haze-gard plus" instrument (BYK Gardner GmbH, Germany). In this test, haze is commonly defined as that portion of visible light that is scattered at wider angles (2.5° < θ < 90°) and is a measure for the turbidity of a sample. Clarity, on the other hand, usually refers to the scattering contribution at small angles (θ < 2.5°) and is related to the sharpness of an object when viewed through the sample (cf. manual of Haze-gard plus).

Thermal Analysis. Thermal analysis was conducted with a Netzsch differential scanning calorimeter (DSC, model 200) with samples of 5−10 mg, unless indicated otherwise at a standard heating or cooling rate of 10 °C/min under nitrogen. Prior to the recording of cooling and heating runs, the samples were held at 240 °C for 5 min to erase thermal history and prevent self-seeding of *i*-PP. Crystallization and melting temperatures hereafter reported refer to peak temperatures in the corresponding DSC thermograms.

Optical Microscopy. Optical micrographs were taken between crossed polarizers with an optical microscope (Leica DMRX) equipped with a hot-stage (Mettler, model FP82TM) at magnifications of 100× and 400×. Cooling and heating rates used for dynamic experiments were 5 °C/min and 10 °C/min, respectively.

Rheology. A universal dynamic spectrometer (Paar Physica UDS 200) was used to measure the temperature dependence of the absolute value of the complex viscosity of various *i*-PP/DMDBS blends in the range 100−220 °C. Disk-shaped specimens (diameter 25 mm, thickness 1 mm) cut from melt-compression molded plaques were used, and the characterization was conducted with a cone−plate setup (40 mm, 6°). Each specimen was initially heated to 220 °C and held for 5 min to achieve thermal equilibrium. A 10% strain was applied at an oscillation frequency of 1 rad/s, and the temperature was subsequently decreased at a rate of 2 °C/min until solidification of *i*-PP occurred.

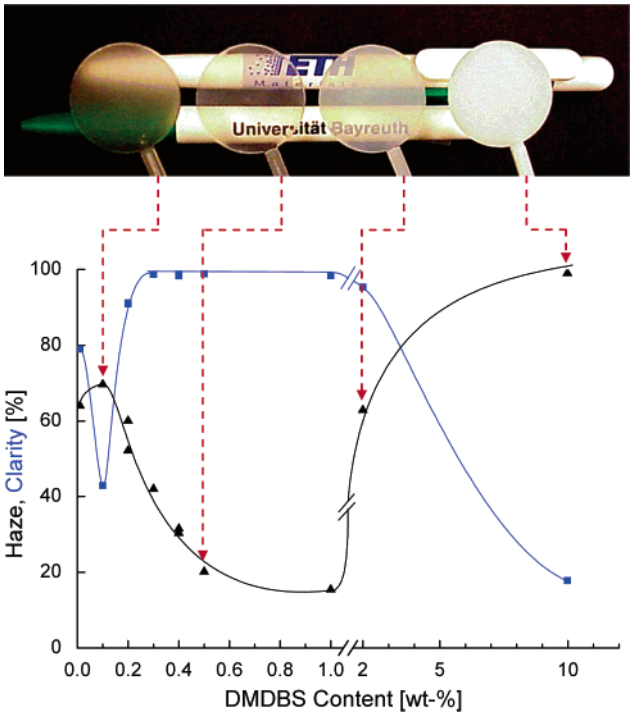

Figure 1. Optical properties of isotactic polypropylene (*i*-PP)/1,3:2,4-bis(3,4-dimethyldibenzylidene)sorbitol (DMDBS) for different compositions. Writing instruments viewed through injection-molded plaques containing 0.1, 0.5, 2, and 10 wt % of DMDBS (top) and measured values for haze (▲) and clarity (■, see text) as a function of the DMDBS content (bottom).

3. Results and Discussion

3.1. Macroscopic Optical Properties. As stated above, by addition of only small amounts of DMDBS (∼0.2 wt %) to *i*-PP, a high clarity of the resulting polymer product may be achieved, which is caused principally by a reduction of the polymer spherulite size due to a dramatic increase in the density of nuclei provided by the additive (cf. ref 23). Figure 1 (top) illustrates this salient effect of the addition of different (minor) amounts of DMDBS on the macroscopic optical properties of injection-molded samples of *i*-PP. In our experiments optimal clarity was achieved at an (initial) additive concentration between 0.2 and 1 wt %. It can also be seen from Figure 1, however, that loss of clarity was observed for samples of additive concentrations exceeding 1 wt %, ultimately leading to complete absence of transmittance of visible light at concentrations of 10 wt % and higher. Figure 1 (bottom) shows the measured values for clarity and haze for *i*-PP comprising different concentrations of DMDBS. Interestingly, a *decrease* in clarity and concomitant *increase* in haze was observed at very low additive concentrations up to about 0.1 wt %. At increasing concentration of DMDBS the clarity of the samples increased and haze decreased up to a critical concentration, which in our experiments was observed to be about 1 wt %. As noted above, samples of higher additive concentrations showed a decreased clarity and dramatically increased haze and, as a matter of fact, displayed the optical appearance of plain paper.

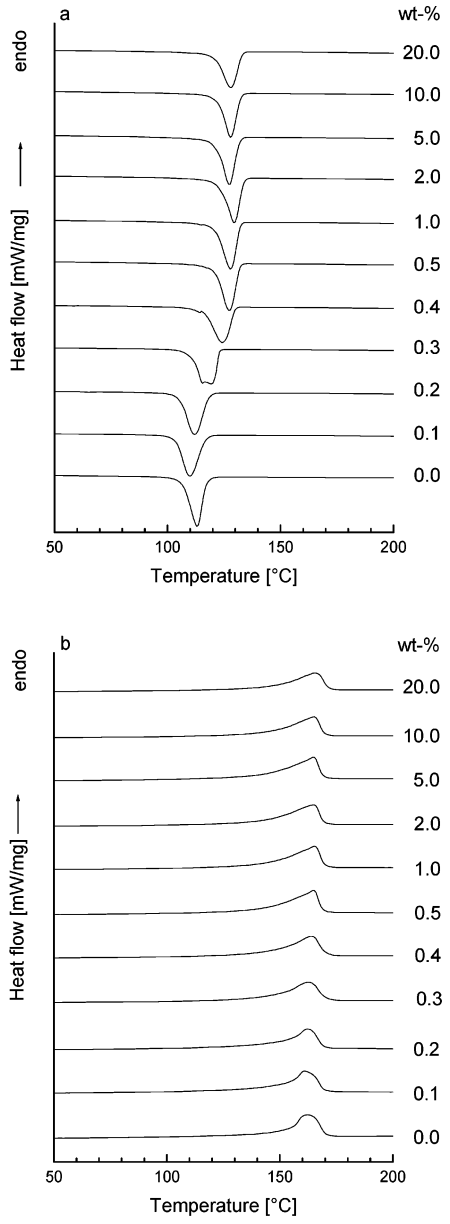

Figure 2. Differential scanning calorimetric (DSC) thermograms of various binary mixtures of *i*-PP/DMDBS melt-compounded at 230 °C: (a) cooling and (b) subsequent heating, both at 10 °C/min.

3.2. Differential Scanning Calorimetry. DSC cooling thermograms of various *i*-PP/DMDBS mixtures are shown in Figure 2a. At very low concentrations of DMDBS the crystallization (peak) temperature of *i*-PP *decreased* slightly from 113 °C for the neat polymer to 110 °C for mixtures containing 0.1 wt % of DMDBS. Thus, it appears that the nucleating/clarifying agent is not effective at very low concentrations, in agreement with earlier observations.[17,18] The latter observation is consistent with the above-noted rise in haze of this particular sample, which will be further discussed hereafter in the context of the entire phase diagram. For *i*-PP/DMDBS compositions containing between 0.1 and 1 wt % of DMDBS the peak crystallization temperature of *i*-PP did rise significantly from 110 to around 129 °C in the mixtures and remained constant at higher DMDBS contents. A detailed overview of the crystallization peak temperatures of low-DMDBS-content mixtures is presented in Figure 3. Three different regimes

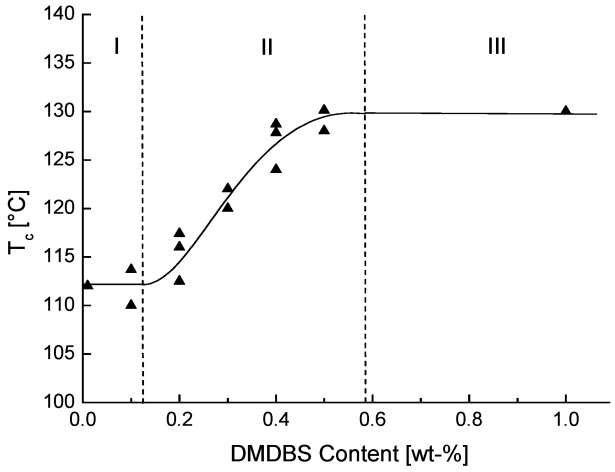

Figure 3. Peak crystallization temperatures vs DMDBS concentration (from DSC data). For denotation of regimes I, II, and III, see text.

can be distinguished in this DMDBS concentration range, here shown up to 1 wt %. As noted above, in regime I DMDBS did, in fact, not act as a nucleating/clarifying agent for *i*-PP. In the very narrow regime II the presence of the additive commenced to cause an increase of the peak crystallization temperature of *i*-PP until it reached a maximum value of about 130 °C and remained constant in regime III. It is noteworthy that the crystallization temperature rises in approximately the same concentration regime where the optical properties of the mixtures were found to improve (cf. Figure 1, bottom).

The addition of DMDBS did hardly affect the melting temperatures of *i*-PP, as can be seen from selected DSC melting thermograms shown in Figure 2b. The recorded values were found between 160 and 165 °C for all samples. Consistent with the corresponding DSC cooling curve, a slight melting point depression was observed at a DMDBS concentration of 0.1 wt %. No significant differences were observed in the degree of crystallinity of *i*-PP in samples of different additive contents. All mixtures exhibited a polymer crystallinity of around 50%, calculated on the basis of a value of 209 J/g[24] for 100% crystalline *i*-PP, corrected for the presence of the additive.

3.3. Rheology. Figure 4 shows the complex viscosity as a function of temperature, recorded during cooling from the melt, for samples containing different amounts of DMDBS. Prior to the experiment the sample was allowed to thermally equilibrate at 220 °C for 5 min to ensure complete melting and to avoid possible self-nucleation of *i*-PP. Typical values of the complex viscosities of molten material at 200 °C were about 200−400 Pa·s in the DMDBS concentration range from 0 to 10 wt %. In the figure the curves were horizontally shifted for clarity of presentation. At low DMDBS concentrations, prior to the nucleation and subsequent crystallization of the polymer, a relatively small but distinct initial increase in viscosity was detected (indicated by the arrows in Figure 4a). Similar observations have been reported previously in the elegant work by Shepard et al.[5] for the system di-*p*-methylbenzylidenesorbitol (MDBS)/*i*-PP for concentrations up to 1 wt % of MDBS. This initial increases in complex viscosity have been shown to be caused by the formation of a nanofibrillar network due to crystallization of the additive in the polymer melt (see e.g. ref 6). In our experiments this

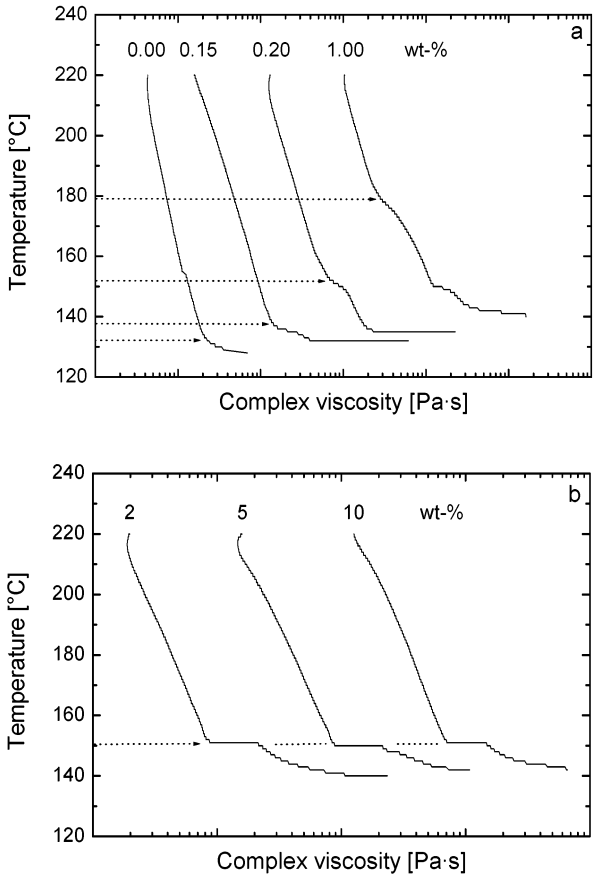

Figure 4. Complex viscosity as a function of temperature upon cooling at 2 °C/min for different *i*-PP/ DMDBS compositions: concentration range 0−1 wt % (a) and 2−10 wt % (b).

shoulder-like, concentration-dependent increase in complex viscosity was observed only in samples of a DMDBS concentration up to 1 wt %. At higher additive concentrations (in Figure 4 shown for 2−10 wt %), by contrast, a sudden sharp increase by a factor of 5 and more in the complex viscosity was observed at 150 °C, virtually independent of the DMDBS concentration. The latter phenomenon we attribute to the presence of eutectic crystallization in the present system which will be discussed later in section 3.5.

3.4. Optical Microscopy. The melting and crystallization behavior of the present *i*-PP/DMDBS system was investigated also by polarized optical microscopy. In Figure 5 are presented photomicrographs of different binary mixtures after cooling from the melt to room temperature at a rate of 10 °C/min. Expectedly, and as can be clearly seen, the resulting morphology strongly depended on the amount of DMDBS present in the mixtures. At DMDBS concentration levels of up to about 0.1 wt % (Figure 5a) the spherulite size of *i*-PP was found to be approximately the same as in neat *i*-PP, again indicating that DMDBS is *not* affecting crystallization of the polymer when present at very low concentrations. As is well-known, at a DMDBS concentrations of for instance 0.2 wt %, a very dramatic decrease in polymer spherulite size was observed (Figure 5b). Similar results have been reported for *i*-PP containing 1,3:2,4-dibenzylidenesorbitol (DBS, Millad 3905) by Garg et al.[25,26] in their light scattering studies. These authors suggested that at very low contents the additive would be inactive either due to destruction by catalyst residues or stabilizers or due to "complete solubility" in the polymer. (Hereafter, we shall offer a simpler, more fundamental explanation for the observed phenomena.) At DMDBS concentrations of more than 5 wt % the appearance of the mixtures was dominated by the presence of large, crystalline DMDBS domains, and only a few polymeric spherulitic structures could be distinguished (Figure 5c).

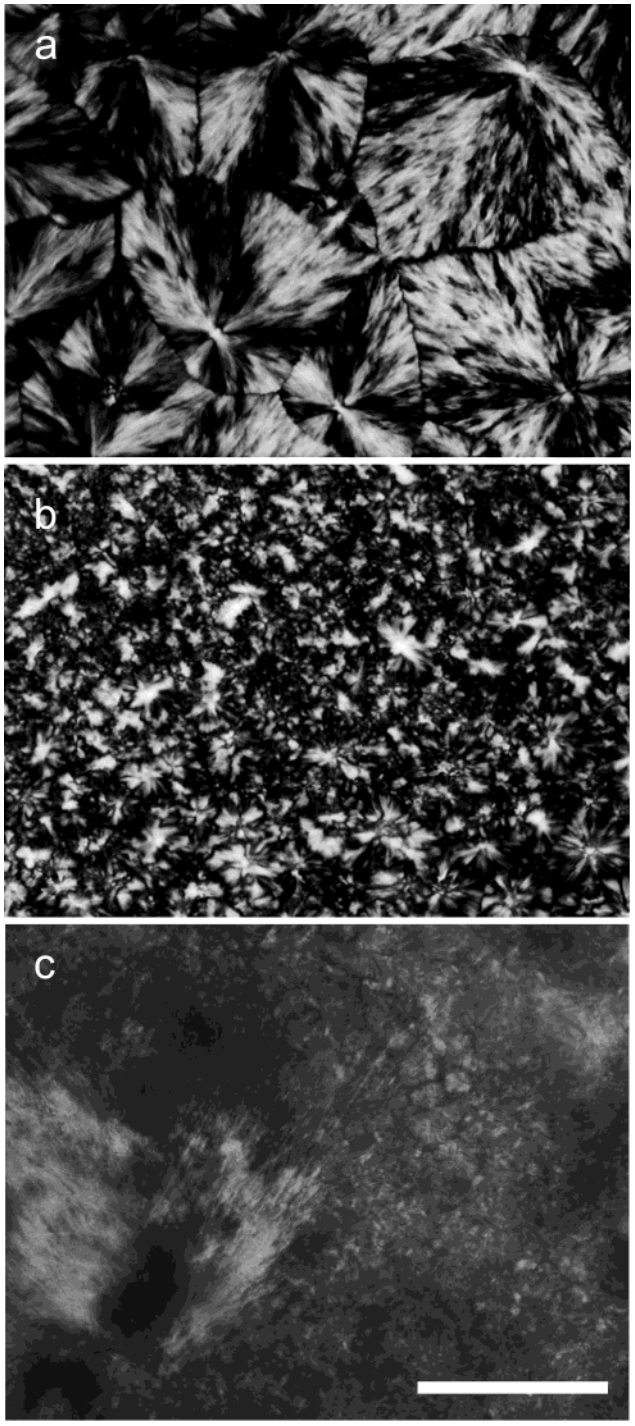

Figure 5. Optical micrographs of the morphology of compression molded films of binary *i*-PP/ DMDBS mixtures containing different amounts of DMDBS (in wt %): (a) 0.1, (b) 0.2, (c) 40.0. Crossed nicols: scale bar 100 μm.

Polarized optical microscopy was employed also to determine melting and crystallization transitions in the various *i*-PP/DMDBS mixtures. The melting points of *i*-PP reported here refer to those temperatures at which no more birefringence arising from the characteristic polymer spherulites could be detected under crossed

polarizers. Values were found to be between 160 and 165 °C for all samples studied, essentially independent of the DMDBS concentration. Samples of mixtures of DMDBS concentrations exceeding 2 wt % above this temperature showed residual birefringent structures in the melt in the form of DMDBS crystals. Importantly, these residual DMDBS crystals were found to dissolve at temperatures around 275 °C, virtually independent of the composition of the binary system over the range of 5−95 wt %. Above the latter temperature liquid−liquid phase separation was observed for mixtures containing more than 2 wt % of DMDBS (cf. Figure 6a). By contrast, mixtures of DMDBS content <2 wt % formed homogeneous, one-phase liquids. Upon cooling the more concentrated, phase-separated liquids, DMDBS was observed to crystallize at temperatures around 245 °C in the form of macroscopic fibrils, as shown in Figure 6b. Upon further cooling at a rate of 10 °C/min, crystallization of *i*-PP occurred at about 130 °C (Figure 6c).

3.5. Temperature/Composition Diagrams. Temperature/composition diagrams for cooling (crystallization) and heating (melting) were constructed from the various experimental data presented above and are shown in the top and bottom of Figure 7, respectively. The resulting diagrams show the general features typical of a simple binary monotectic, which commonly is found for mixtures of two species of limited liquid miscibility and a high immiscibility in the solid state. Even a cursory comparison between the two diagrams reveals relatively large differences between melting and crystallization temperatures of the components in the present system, which is indicative of the highly nonequilibrium nature of the diagrams. Consequently, important effects of kinetics on the location of the various liquidus curves and the monotectic and eutectic temperatures as well as on the structure and properties of the resulting solids are to be expected. Illustrative in this respect is, for instance, that the eutectic crystallization temperature—due to the nucleating ability of the additive—is, in fact, *above* the crystallization temperature of the neat polymer. Another indication of the strong influence of kinetics on the diagram is that the eutectic crystallization temperature when measured at a cooling rate of 10 °C/min (DSC, ●) is found at around 130 °C, while it is located as high as about 150 °C in cooling experiments conducted at 2 °C/min (rheology, ★).

In the following we discuss the advanced monotectic phase behavior of the *i*-PP/DMDBS system, especially in the context of the observed, remarkable composition-dependent variation of the optical properties. For this purpose a highly schematic, simple binary monotectic phase diagram is presented in Figure 8. Broadly speaking, four distinct composition regimes can be recognized, here denoted by the Roman numbers I−IV.

In the very low-additive-content regime I (i.e., below the eutectic composition marked "e"), upon cooling the homogeneous liquid (L_1 in Figure 7) the polymer crystallizes *prior* to the additive, and the latter is, in fact, not substantially affecting the crystallization behavior of the polymer. In this regime we expect a slight depression of the crystallization temperature of the polymer due to the presence of the dissolved additive. This behavior was, in fact, detected in *i*-PP mixtures containing <0.1 wt % of DMDBS and explains the (minor) increase in haze observed for mixtures of such compositions. In other words, DMDBS is inactive as a nucleating and clarifying agent when present at very low concentrations, not because of destruction of the additive, but simply because it acts merely as a high-melting (poor) solvent in the relevant temperature regime.

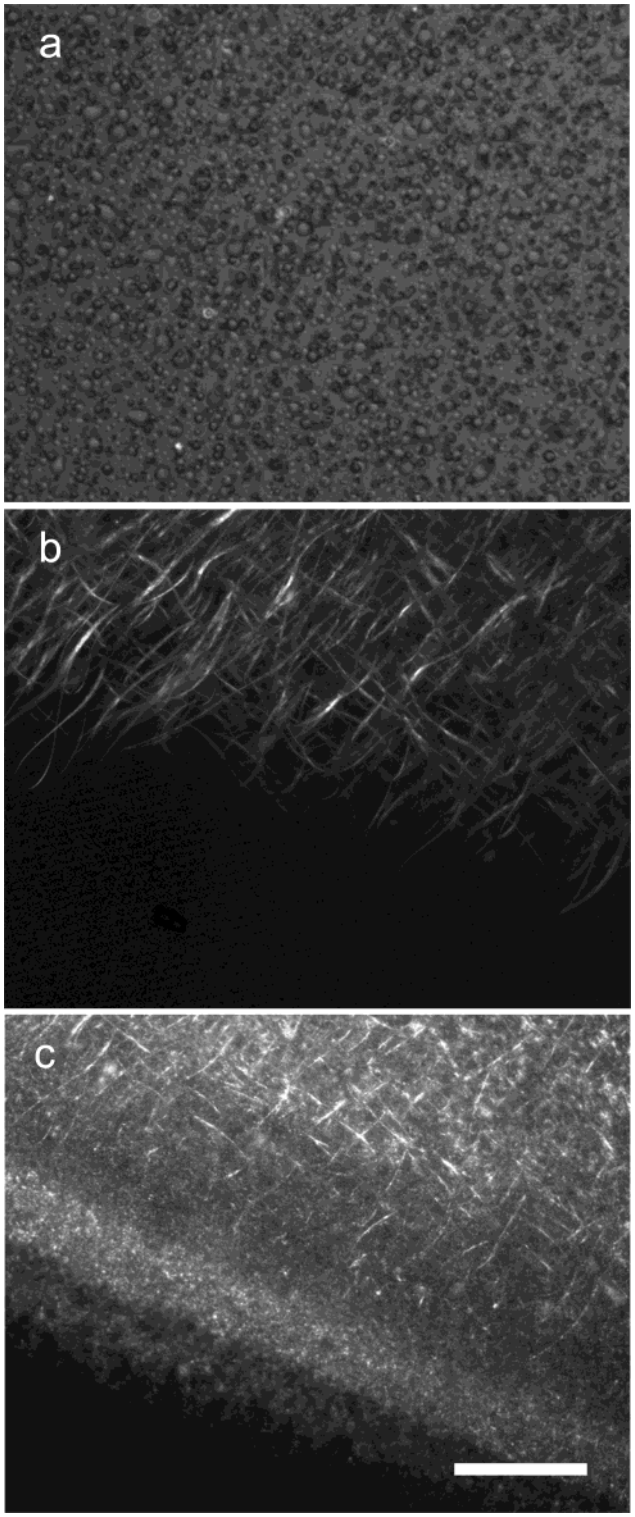

Figure 6. Optical micrographs of a binary *i*-PP/DMDBS mixture containing 5 wt % of DMDBS showing: (a) liquid−liquid phase separation (picture taken at 277 °C); (b) crystallization of DMDBS (picture taken at 220 °C); (c) morphology at room temperature. Crossed nicols: scale bar 200 μm; (b, c) lower left corner is edge of sample.

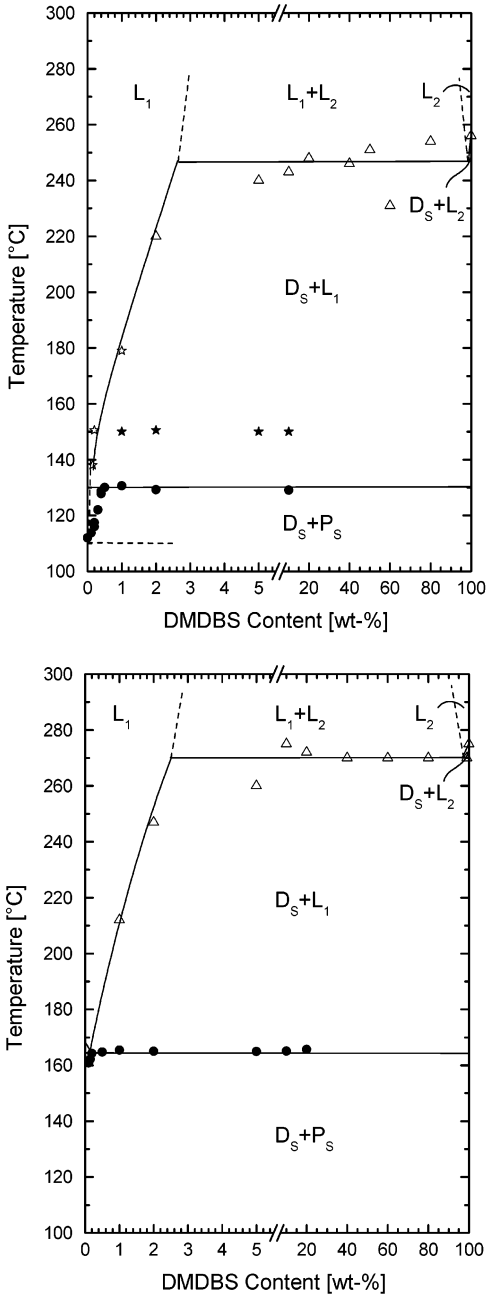

Figure 7. Crystallization (top) and melting (bottom) temperature/composition diagrams of the binary system *i*-PP/DMDBS. In the diagrams the symbols refer to experimental data obtained by (●) DSC, (★/☆) rheology, and (△) optical microscopy. The denotation D refers to DMDBS, P to *i*-PP, L to liquid, and S to solid.

In the very high concentration regime IV above the monotectic "m", DMDBS crystallizes prior to the polymer upon cooling the homogeneous liquid (Figure 7, L_2), and a slight melting point depression caused by minor amounts of dissolved *i*-PP is expected. In this composition regime the morphology of the solidified mixture is dominated by the large primary structures formed by the additive.

In the relatively broad concentration regime III, above the monotectic temperature no homogeneous liquid exists, but liquid−liquid phase separation is observed. Upon cooling this phase-separated liquid, DMDBS crystallized below the monotectic temperature into large fibrillar structures which were readily visible in the optical microscope, followed by the solidification of *i*-PP

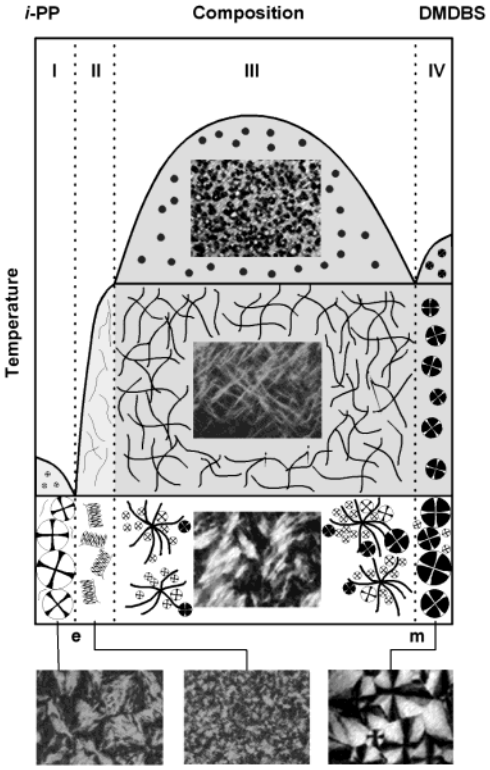

Figure 8. Proposed schematic, monotectic phase diagram of the binary system *i*-PP/DMDBS. Indicated are four relevant composition ranges (see text) and inserted are sketches and actual optical micrographs (crossed nicols) of the various states of matter of representative mixtures of compositions in those ranges.

below the much lower, invariant eutectic temperature, as was observed experimentally. In this regime, already in the fluid phase, the additive is assembled into relatively large domains through the process of liquid−liquid phase separation, which ultimately leads to structures that very significantly scatter visible light, leading to poor clarity and haze of the solid mixtures.

The concentration region of main interest (and use) is regime II where the polymer and the additive form a homogeneous liquid L_1 at temperatures above the so-called "lower liquidus". Upon cooling this homogeneous liquid, the additive crystallizes prior to the polymer without a preceding separation into two liquids. Thereby the additive forms (submicron-sized) structures in the polymer-rich liquid. This behavior manifested itself in the form of an initial increase in the complex viscosity upon cooling the binary *i*-PP/DMDBS liquid L_1 to temperatures below the lower liquidus. The resulting, finely crystallized additive provides an extremely large surface of active nucleation sites, giving rise to a substantial increase in the peak crystallization temperature of the polymer in this regime. As a consequence, when compared to structures formed in regime III, due to the absence of a liquid−liquid phase separation in regime II, the final morphology of the *i*-PP/DMDBS mixtures exhibits much smaller crystalline entities which lead to a substantial decrease in the scattering of visible light and, thus, to an improvement of the optical properties.

3.6. Influence of Cooling Rate. As noted above, and also previously reported, among others, by Martin et al.[16] in their study of a propylene/ethylene copolymer and an (unspecified) sorbitol-based clarifier, we observed that the crystallization behavior and optical properties

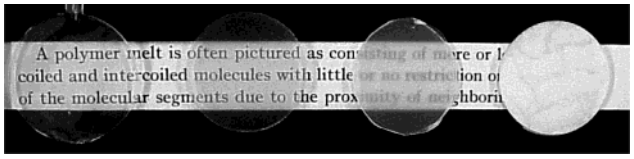

Figure 9. Illustration of the effect of the cooling rate on the macroscopic optical properties on a melt-compressed *i*-PP/DMDBS mixture comprising 1.0 wt % of DMDBS (from left to right): injection molded (a), quenched in a cold press (b), cooled at approximately 10 °C/min (c), cooled at about 10 °C/h (d). Note that sample d, when remelted at 240 °C and quenched (in a cold press), had the same appearance as sample b.

of the present *i*-PP/DMDBS system also significantly depended on the processing conditions, in particular on the rate of solidification. The above-discussed temperature/composition diagrams were determined at cooling rates in the relatively narrow range from 2 °C/min (rheology) to 10 °C/min (microscopy and calorimetry). In a brief, illustrative excursion we also explored the effect of cooling rate on the optical properties over a much wider range. When decreasing the rate of solidification of samples containing 1 wt % of DMDBS from that occurring in injection molding (of the order of 100 °C/s), quenching in a cold press (about 10 °C/s), cooling at 10 °C/min to 10 °C/h, the samples displayed a remarkably strong increased haze and become fully opaque at the latter cooling rate (Figure 9). Importantly, the above degradation of the optical properties could be reversed simply by remelting of the mixture and recrystallizing it at the appropriate cooling rate. Even after extremely slow cooling (10 °C/h), which resulted in a plain white object (cf. Figure 9d), optical clarity could be regained upon remelting and subsequent fast cooling. The latter observation implies that slow cooling did not result in thermal decomposition of the clarifying agent. Evidently, the strong dependence of the cooling rate on the optical properties of the *i*-PP/DMDBS system has important practical consequences. For instance, the observed reduction of desirable optical properties with decreased cooling rate is likely to preclude manufacturing of "clarified" articles of large thickness with conventional processing techniques.

4. Conclusions

In this work we propose a monotectic phase diagram for the binary system consisting of isotactic polypropylene and the nucleating/clarifying agent 1,3:2,4-bis(3,4-dimethylbenzylidene)sorbitol. This suggested phase behavior is consistent with the experimental data and provides a logical, simple base for understanding the seemingly complex dependence of the thermal and optical properties of *i*-PP/DMDBS mixtures on their composition. The presented insight may facilitate the search and development of a broader range of "clarifying" agents for *i*-PP as well as for other crystallizable polymers.

Acknowledgment. Sandra Ganzleben (University of Bayreuth, Germany) is acknowledged for her valuable assistance in sample preparation.

References and Notes

(1) Hamada, K.; Uchiyama, H. US Pat. 4,016,118. Mahaffey, R. L. US Pat. 4,371,645. Mahaffey, R. L. US Pat. 4,419,473. Machell, G. US Pat. 4,562,265. Rekers, J. W. US Pat. 5,049,-605. Mannion, M. J. US Pat. 5,198,484.
(2) Fillon, B.; Lotz, B.; Thierry, A.; Wittmann, J. C. *J. Polym. Sci., Polym. Phys.* **1993**, *31*, 1395−1405.
(3) Thierry, A.; Straupé, C.; Lotz, B.; Wittmann, J. C. *Polym. Commun.* **1990**, *31*, 299−301.
(4) Binsbergen, F. L. *Polymer* **1970**, *11*, 253−267.
(5) Shepard, T. A.; Delsorbo, C. R.; Louth, R. M.; Walborn, J. L.; Norman, D. A.; Harvey, N. G.; Spontak, R. J. *J. Polym. Sci., Polym. Phys.* **1997**, *35*, 2617−2628.
(6) Maier, R. Thermodynamik und Kristallisation von Metallocen-Polyolefinen. Ph.D. Thesis, Freiburg i. Br., Germany, 1999.
(7) Ilzhoefer, J. R.; Spontak, R. J. *Langmuir* **1995**, *11*, 3288−3291.
(8) Fahrländer, M.; Fuchs, K.; Friedrich, C. *J. Rheol.* **2000**, *44*, 5, 1103−1119.
(9) Mercurio, D. J.; Spontak, R. J. *J. Phys. Chem. B* **2001**, *105*, 2091−2098.
(10) Mercurio, D. J.; Saad, A. K.; Spontak, R. J. *Rheol. Acta* **2001**, *40*, 30−38.
(11) Mitra, D.; Misra, A. *Polymer* **1988**, *29*, 1990−1994.
(12) Nahir, T. M.; Qiu, Y.-J.; Williams, J. L. *Electroanalysis* **1994**, *6*, 972−975.
(13) Smith, J. M.; Katsoulis, D. E. *J. Mater. Chem.* **1995**, *5*, 11, 1899−1903.
(14) Silva, F.; Sousa, M. J.; Pereira, C. M. *Electrochim. Acta* **1997**, *42*, 3095−3103.
(15) Janssen, R. C.; Stümpflen, V.; Broer, D. J.; Tervoort, T. A.; Smith, P. *J. Appl. Phys.* **2000**, *88*, 161−167.
(16) Martin, C. P.; Vaughan, A. S.; Sutton, S. J.; Swingler, S. G. *J. Polym. Sci., Polym. Phys.* **2002**, *40*, 2178−2189.
(17) Marco, C.; Ellis, G.; Gomez, M. A.; Arribas, J. M. *J. Appl. Polym. Sci.* **2002**, *84*, 2440−2450.
(18) Hoffmann, K.; Huber, G.; Mäder, D. *Macromol. Symp.* **2001**, *176*, 83−91.
(19) Zhao, Y.; Vaughan, A. S.; Sutton, S. J.; Swingler, S. G. *Polymer* **2001**, *42*, 6587−6597.
(20) Nagarajan, K.; Myerson, A. S. *Cryst. Growth Des.* **2001**, *1*, 131−142.
(21) Mathieu, C.; Thierry, A.; Wittmann, J. C.; Lotz, B. *Polymer* **2000**, *41*, 7241−7253.
(22) Smith, T. L.; Masilamani, D.; Bui, L. K.; Khanna, Y. P.; Bray, R. G.; Hammond, W. B.; Curran, S.; Belles, J. J., Jr.; Binder-Castelli, S. *Macromolecules* **1994**, *27*, 3147−3155.
(23) Thierry, A.; Fillon, B.; Straupé, C.; Lotz, B.; Wittmann, J. C. *Prog. Colloid Polym. Sci.* **1992**, *87*, 28−32.
(24) *Polymer Handbook*, 3rd ed.; Bandrup, J., Immergut, E. H., Eds.; Wiley-Interscience: New York, 1989; Vol. 29, p V-31.
(25) Garg, S. N.; Stein, R. S. *ANTEC* **1988**, 1021−1025.
(26) Garg, S. N.; Stein, R. S.; Su, T. K.; Tabar, R. J.; Misra, A. In *Kinetics of Aggregation and Gelation*; Family, F., Landau, D. P., Eds.; North-Holland: Amsterdam, 1984; p 229.

MA030146T